Role of confinement and aggregation in charge transport in semicrystalline polythiophene thin films

Duc T. Duong,[1] Michael F. Toney,[2] and Alberto Salleo[1]
[1]*Department of Materials Science and Engineering, Stanford University, Stanford, California 94305, USA*
[2]*Stanford Synchrotron Radiation Lightsource, SLAC National Accelerator Laboratory, Menlo Park, California 94025, USA*
(Received 14 August 2012; published 27 November 2012)

Crystallite orientations, molecular packing disorder, and hole mobility of poly(3-hexylthiophene) thin films that are spin casted from different solvents are studied as a function of film thickness. Grazing incidence x-ray diffraction reveals that films consist of an ultrathin layer of ordered, edge-on oriented aggregates and a more disordered, face-on oriented bulk region. Diffraction and optical absorption spectroscopy elucidate the film-forming process. Field-effect hole mobility provides evidence for interconnecting aggregates as the mechanism for efficient charge transport.

DOI: 10.1103/PhysRevB.86.205205 PACS number(s): 81.05.Fb, 68.55.am

Semiconducting polymers are of increasing interest due to their potential in the fabrication of low-cost, solution-processable thin-film transistors, light-emitting diodes, and photovoltaics.[1–5] These polymers are semicrystalline in nature and, in thin films, tend to form ordered domains consisting of cofacially stacked π-conjugated chain backbones dispersed within an amorphous matrix.[6] While the performance of semiconducting polymers has approached that of amorphous silicon, it is difficult to comprehensively describe the solid-state microstructure due to the inherent materials' complexity. For inorganic semiconductors such as silicon or GaAs, the relationship between electronic properties (i.e., charge carrier density, carrier mobility) and structural properties (i.e., atomic structure, doping density) is well understood.[7] This is not the case for organic semiconductors and the physical structure through which charge carriers propagate is only partly understood. This lack of knowledge on film microstructure makes it difficult to rationally design new polymers: Tailoring the molecular structure is not sufficient. The nature of the crystalline structure and the fraction of ordered regions in the film also affect electronic performance. We must be able to understand the film forming process, characterize the overall morphology—with particular attention paid to the structure of ordered and disordered regions—and understand how charges propagate across the proposed microstructure.

One of the most studied semiconducting polymers is poly(3-hexylthiophene) (P3HT). Due to the abundance of available experimental data,[8–12] P3HT is considered a model high-performance semiconducting polymer and will be the focus of our study. The fundamental goal is to correlate the microstructure and morphology of P3HT to its electronic properties. Although several reports have investigated charge transport of polythiophenes in solution-processed thin films as a function of physical properties and processing conditions, the results are often *qualitative* and a complete description of the film structure is needed.[13–15] In order to carefully analyze semiconducting polymer thin films, the microstructures of both the bulk of the film and the buried interface should be decoupled and *quantitatively* described with minimal physical disruptions. Furthermore, to engineer better processing conditions the course of film formation must be well understood.

We investigate the anisotropic morphology and film formation of spin-cast P3HT thin films from 1,2-dichlorobenzene (DClb), chlorobenzene (Clb), and chloroform (Clf) using quantitative interpretations of x-ray diffraction and linear optical absorption experiments. We find that film formation begins with the rapid growth of a highly ordered interfacial layer, followed by the slow crystallization of thermodynamically favored, edge-on aggregates from the substrate-polymer interface and fast precipitation of kinetically favored, face-on aggregates from the bulk solvent. Our results allow us to differentiate between the microstructures of the bulk and the interface and clearly elucidate the relationship between interface film microstructure and charge transport. We further demonstrate that major changes in the bulk film may not significantly affect the interface microstructure and thereby the field-effect mobility. A comparison of quantitative microstructural analysis and hole mobility measurements extracted from field-effect transistors (FETs) shows that charge transport is controlled by interconnected aggregates.

First, we define an "aggregate" as a group of π-stacked conjugated segments [Fig. 1(a)] giving rise to specific photophysical properties, as previously described.[16–18] If an aggregate is composed of enough π-conjugated segments, they will produce discernible diffraction peaks. There can always exist, however, aggregates that are too small to diffract (e.g., dimers and trimers). In this paper we will correlate structural properties of aggregates captured by x-ray diffraction to photophysical properties observed using absorption spectroscopy. We make the assumption that changes in the orientation of *diffracting aggregates* reflect changes in the *entire* aggregate population and will use the term "aggregate" to refer to both diffracting and nondiffracting species. We deem this to be a good assumption based on the fact that all aggregates of the same orientation (e.g., face on or edge on) most likely nucleate in the same manner. Finally, we will use the term "crystallite" to refer to aggregates that participate in lamellar stacking. Thus a crystallite contains aggregates but not all aggregates are in crystallites.

We investigate the structural properties of P3HT thin films ($M_w = 105$ kDa, $M_n = 60$ kDa) by performing grazing x-ray incidence diffraction (GIXD). Indexed lamellar (100) and π-π (010) spacings of $\sim$16.5 and $\sim$3.83 Å are consistent with previous reports for P3HT.[12,19,20] The two-dimensional (2D) diffraction patterns also show the coexistence of both in-plane and out-of-plane π-stacking peaks, corresponding

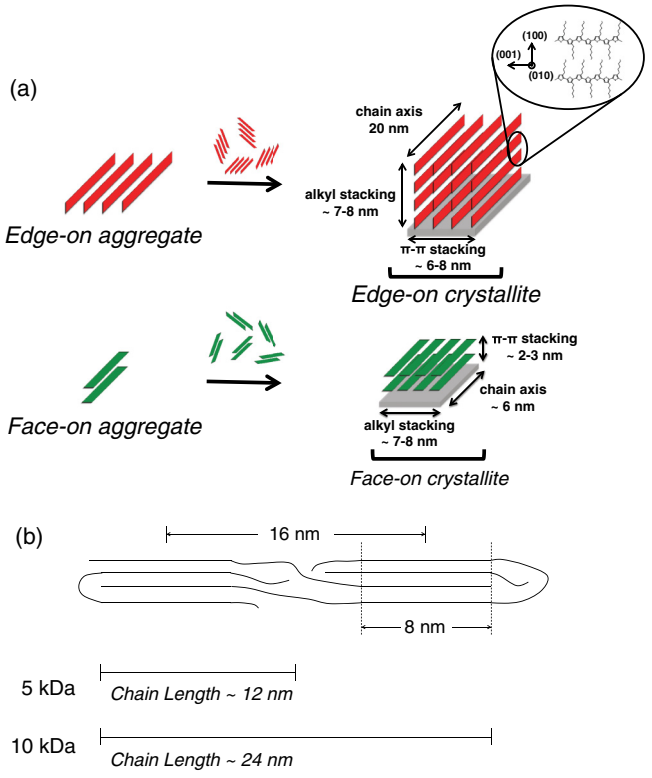

FIG. 1. (Color online) (a) Sketches of edge-on and face-on aggregates and crystallites along with their respective conjugation and coherence lengths. The aggregates shown here exhibit excitonic absorption bands as described by the Spano analysis and are expected to also diffract. (b) Critical polymer chain lengths for interconnected aggregates.

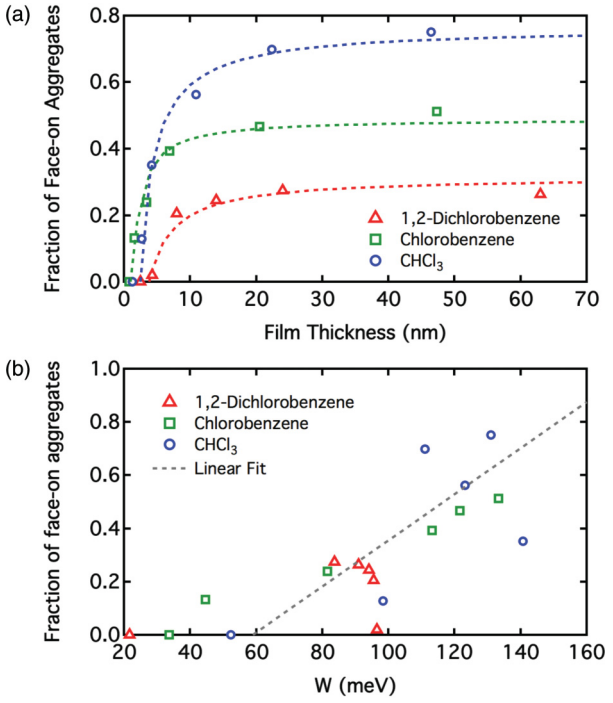

FIG. 2. (Color online) (a) Fractions of face-on aggregates in P3HT thin films that are spin casted from three different solvents as a function of film thickness. Fits to the bilayer aggregate model are shown as dotted lines. (b) Overall fraction of face-on aggregates as a function of excitonic bandwidth W and the corresponding linear fit yielding $W \sim 140$–200 meV for face-on and $W \sim 40$–80 meV for edge-on aggregates. The range of values is attributed to scatter in the data. W is also inversely related to the solvent boiling point, similar to Ref. 18.

to edge-on and face-on crystallites, respectively. We have quantified the fraction of face-on aggregates, defined by the number of face-on aggregates divided by the total number of aggregates, by comparing the diffracted intensity of the π-stacking peaks for the two different orientations (see the Supplemental Material for 2D patterns and a description of the quantitative method[21]). The results, summarized in Fig. 2(a), show that for all three solvents the texture of the aggregates becomes increasingly edge on as the film thickness decreases. In addition, the fraction of face-on aggregates is larger when P3HT is spin cast from a lower boiling point solvent (Cf) and approaches zero in all cases for films on the order of 1–2 nm. We fit our data to a bilayer aggregate model described by $Ft_{\text{tot}} = F_i t_i + F_B(t_{\text{tot}} - t_i)$, where F_i and F_B represent the fraction of face-on aggregates at the interface and in the bulk, respectively, t_i is the thickness of the interfacial layer, and t_{tot} is the total film thickness. Here we assume that the thickness of the interfacial layer and the different fractions of face-on aggregates are independent of film thickness. We deem this to be a good assumption based on the fact that the polymer films grow in a bottom-up fashion (as later presented in our crystallization model) and, as such, the interface layer is weakly coupled to the bulk. The fits are plotted as dotted lines [Fig. 2(a)]. The results of the fits show that F_i is nearly zero for films that are spin cast from different solvents, F_B increases as the solvent boiling point decreases (0.32 for DClb, 0.49 for Clb, and 0.76 for Cf), and t_i ranges from 1.3 to 3.7 nm. Although our bilayer model is insensitive to whether the interfacial layer resides at the substrate-polymer interface or at the polymer-air interface, we expect the former to be true due to previous work by Kline *et al.*[22] Furthermore, we observe more intrachain order in ultrathin films of P3HT (<5 nm) when the substrate is treated with hexamethyldisilazane (HMDS) (*vide infra*), which supports the conclusion that the ordered layer crystallizes at the substrate-polymer interface. These observations suggest that P3HT films consist of an ultrathin layer of edge-on aggregates at the substrate-polymer interface and a bulk region that contains more face-on aggregates.

We also collected optical absorption spectra of P3HT thin films. The data are fitted according to a modified aggregate model developed by Spano *et al.*[23] The parameters of interest in this fit are the excitonic bandwidth W, which is related to the degree of disorder along the polymer chain backbone within an aggregate, and the percent aggregate. A higher W corresponds to larger intrachain disorder and thereby shorter conjugation lengths. Our data show that W is inversely related to the solvent boiling point, as was previously reported by Clark *et al.*[18] (see the Supplemental Material[21]). By relating the fraction of face-on aggregates from x-ray diffraction with W determined by the Spano analysis, we extrapolate values for W of ~140–200 and ~40–80 meV for face-on and edge-on aggregates, respectively, based on a simple linear fit to the data

in Fig. 2(b). Note that, by performing this linear fit, we do not suggest that the absorption spectra are composed of a linear combination of edge-on and face-on aggregate absorption. Rather, it is a simple way for us to estimate the difference in excitonic bandwidths between the two species. According to the model by Gierschner *et al.*,[24] these values correspond to conjugation lengths of ∼15 repeat units (6 nm) and ∼50 repeat units (20 nm), respectively. Furthermore, by measuring the diffraction peak widths,[25] we estimate the coherence lengths along the π-π stacking direction to be ∼2–3 nm for face-on aggregates and ∼6–8 nm for edge-on aggregates. Interestingly, when these aggregates are alkyl stacked to form crystallites they exhibit similar lamellar coherence lengths of ∼7–8 nm of the (100) planes regardless of texture. Figure 1(a) provides a visual description of the two different types of crystallites. These results show that face-on crystallites are inherently more disordered than their edge-on counterpart in the π-stacking direction and along the chain backbone. We expect this difference to hold true for most semiconducting polymers.

X-ray diffraction and optical absorption experiments also shed light on the kinetics of film formation by solution processing. The first step in thin-film formation most likely involves the fast heterogeneous nucleation of an ultrathin layer of edge-on aggregates at the substrate-polymer interface. This hypothesis is supported by the small excitonic bandwidths observed in all ultrathin (∼1–2 nm) films of P3HT regardless of the host solvent (see the Supplemental Material[21]). Furthermore, heterogeneous nucleation is known to depend strongly on the surface energy of the substrate. Thus, we have collected absorption spectra for P3HT films of different thicknesses deposited on both plain and HMDS-treated glass [the P3HT used for this particular experiment is of a lower molecular weight, $M_w = 20$ kDa and $M_n = 25$ kDa, and cannot be directly compared to Fig. 2(a)]. Fitting our data to the aggregate model reveals that films of similar thicknesses on either substrate exhibit the same excitonic bandwidths except for the thinnest film (4.7 nm), where the HMDS-treated film is more ordered [Fig. 3(a)]. This result suggests that surface treatment only improves the structural and electronic order within the first two to three aggregate layers in P3HT while leaving the bulk of the film unaffected (similar to Ref. 22). In the second stage of film formation, we propose a dual crystallization model wherein highly ordered, edge-on aggregates nucleate off the previously described interfacial layer, as suggested by the high percentage (nearly 100%) of edge-on aggregates near the dielectric interface (as previously described by our two-layer model), while simultaneous rapid solvent evaporation drives the nucleation of more disordered, face-on aggregates out of solution. Previous kinetic studies of film solidification by Sanyal *et al.*[26] show the formation of out-of-plane lamellar stacking [specifically the (h00) series] well before the appearance of any other characteristic P3HT peaks during solvent evaporation. To test these hypotheses we have obtained GIXD data for P3HT films fabricated by spin casting a polymer solution at increasing spin speeds, which increases the solvent evaporation rate. Analyses of these films show that the fraction of face-on aggregates increases as a function of spin speed [Fig. 3(b)]. Faster evaporation rates therefore reduce the time needed for slow growths of edge-on

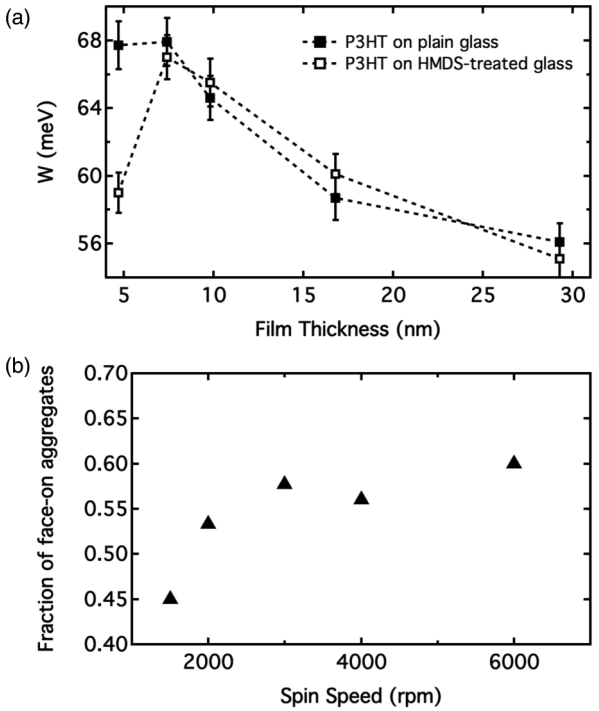

FIG. 3. Effects of surface treatment and evaporation on film morphology: (a) Excitonic bandwidths of P3HT films on plain and HMDS-treated glass substrates and (b) fraction of aggregates of P3HT films that are spin cast from Clb at different spin speeds. Data in (a) are from a lower molecular weight P3HT ($M_w = 20$ kDa).

aggregates at the dielectric interface, leading to a higher percentage of polymer chains forming face-on aggregates into the bulk region. DeLongchamp *et al.* previously reported a similar increase in face-on orientation with higher spin speed in the top ∼10 nm of P3HT thin films.[27]

We hypothesize that lamellar-stacked crystallites are not nucleated directly from soluble P3HT chains but form via *in situ* organization of preexisting aggregates in the wet film. This hypothesis is supported by several key observations. First, the alkyl stacking coherence lengths are essentially the same for both edge-on and face-on crystallites, which suggests that the mechanism for associating alkyl chains is the same in both cases. Second, from our fits to the absorption spectra we observe that the aggregate fraction does not vary significantly as a function of solvent or film thickness. Recent investigations into the thickness-dependent morphology of P3HT, however, indicate that the volume fraction of *crystallites* decreases as the films become thinner.[28] As a result, we conclude that in the "noncrystalline" part of P3HT films, where lamellar stacking does not occur, there must be aggregates. We can infer then that P3HT chains from solution first nucleate into aggregates, which then further organize into three-dimensional crystallites. We suspect that an independent layer at the polymer-air interface also exists and several studies have attempted to characterize its structural and electronic properties, though the results are not conclusive.[29,30] As such we do not attempt to model the top interface. The proposed model for film formation is summarized in Fig. 4.

We now wish to correlate our microstructural studies with charge transport in P3HT films by fabricating bottom

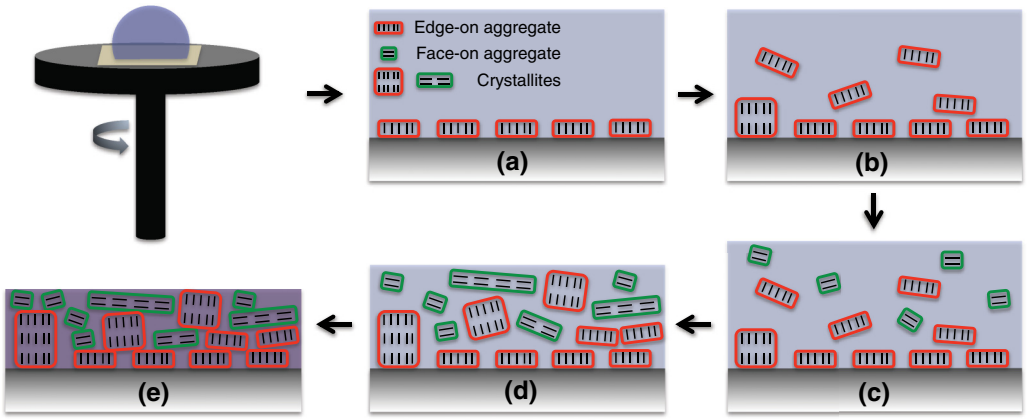

FIG. 4. (Color online) Proposed mechanism for P3HT solidification. Following the establishment of a solvent sheet by spin casting, an ultrathin interfacial layer of edge-on aggregates forms at the substrate-polymer interface (a). As the solvent evaporates, more edge-on aggregates nucleate off the wetting layer (b), face-on aggregates nucleate from either the polymer-air interface or in the bulk (c), and aggregates can self-assemble into lamellar-stacked crystallites (d). Once the film has dried, the final morphology consists of a mostly edge-on interface with a mixture of both face-on and edge-on aggregates and crystallites in the bulk (e).

gate FETs of P3HT films with top gold contacts. The thickness-dependent, field-effect mobilities have been previously discussed[15,31] and will be more thoroughly addressed in a separate study. Here we analyze solvent effects on charge transport in thick films of P3HT. The mobility for thick films increases by only about a factor of 2 as the boiling point of the spin-casting solvent is increased from 61 °C for Cf [$\mu \sim 4.4 \times 10^{-4}$ cm^2(V s)$^{-1}$] to 180 °C for DClb [$\mu \sim 1.1 \times 10^{-3}$ cm^2(V s)$^{-1}$]. This is consistent with previous results reported by Kline *et al.*[32] Our model for film formation can explain this observation. Although the total fraction of face-on aggregates changes significantly between these solvents, the accumulation layer where charge transport occurs in organic thin-film transistors (TFTs) is on the order of a few nanometers,[33–35] which comprises only one to two layers of aggregates. Since the aggregate layer closest to the substrate is nearly completely edge on for all films, the total fractions of face-on aggregates for *the first two layers* are ∼0% and ∼22% for films that are spin cast from dichlorobenzene and chloroform, respectively. Thus, aggregates in the conducting channel are mostly edge on (>50%) and we expect that there exist percolating networks of edge-on aggregates near the substrate-polymer interface in both cases (*vide infra*). Therefore we propose that charge transport occurs via interconnecting aggregates and that the propagation of carriers through well-ordered edge-on aggregates is more efficient than through disordered face-on aggregates, consistent with Ref. 11. It is important to note that when comparing bottom-gated FET mobilities to thin-film morphologies, the interfacial layer is of utmost importance and information extracted from surface or bulk characterization techniques may not be able to explain the observed charge transport.

To further validate this conclusion, we have analyzed a recent report by Reid *et al.*[36] on the molecular-weight dependence of absorption in P3HT. By using the reported excitonic bandwidths and percent aggregates, we define the dimensions for P3HT aggregates at different molecular weights and the average distance between aggregates (defined as the long spacing according to Ref. 23). Here we only consider transport through edge-on aggregates. From these calculations, we show in Fig. 1(b) that above a molecular weight of ∼10 kDa a single polymer chain can bridge two isolated aggregates. The extrapolated values for the long spacing and interacting length agree well with previously reported transmission electron microscopy data.[37] In addition, the mobility of P3HT has also been observed to increase by an order of magnitude at molecular weights around 10 kDa and saturates above ∼30 kDa.[8,38] Finally, a recent report by Collins *et al.*[39] shows that a longer orientation correlation length (OCL) in a high-performance polythiophene leads to much improved field-effect mobilities. Improving the OCL has the effect of increasing the distance over which polymer backbones remain straight and parallel to each other, which increases the likelihood for both aggregate formation and the bridging of isolated aggregates by polymer chains. We can thus conclude that high mobility in P3HT can be obtained as long as ordered aggregates are properly bridged by long polymer chains.

In this paper we have shown that the microstructure of P3HT thin films consists of an ultrathin, interfacial layer of edge-on aggregates covered by a more disordered, face-on bulk film. We propose a mechanism for aggregate nucleation, crystallite assembly, and film formation. We conclude that efficient transport occurs mostly within the observed interfacial layer and requires good interconnectivity between well-ordered aggregates. Our findings therefore provide a coherent picture of the nanoscale morphology for P3HT thin films and can be used for the general design of materials for electronic devices. The ability to nucleate well-ordered, extended π-stacked aggregates off the substrate-film interface, for instance, is more important for FET applications than the inherent crystallinity of a particular polymer. These findings should also serve to change how researchers approach issues of microstructure-dependent charge transport in semiconducting polymers.

A.S. gratefully acknowledges financial support from the National Science Foundation in the form of a CAREER

award. D.T.D. is supported by a Stanford Graduate Fellowship and the National Science Foundation Graduate Research Fellowship. A portion of this research was carried out at the Stanford Synchrotron Radiation Lightsource, a national user facility operated by Stanford University on behalf of the US Department of Energy, Office of Basic Energy Sciences. We kindly thank I. McCulloch and M. Heeney (Imperial College, U.K.) for samples of P3HT.

[1] A. Facchetti, Mater. Today **10**, 28 (2007).
[2] J. Shinar and R. Shinar, J. Phys. D: Appl. Phys. **41**, 133001 (2008).
[3] C. J. Brabec and J. R. Durrant, MRS Bull. **33**, 670 (2008).
[4] G. Li, R. Zhu, and Y. Yang, Nat. Photonics **6**, 153 (2012).
[5] S. W. Yun, J. H. Kim, S. Shin, H. Yang, B.-K. An, L. Yang, and S. Y. Park, Adv. Mater. **24**, 911 (2012).
[6] A. Salleo, Mater. Today **10**, 38 (2007).
[7] S. M. Sze and K. K. Ng, *Physics of Semiconductor Devices* (Wiley-VCH, Hoboken, NJ, 2007).
[8] J.-F. Chang, J. Clark, N. Zhao, H. Sirringhaus, D. W. Breiby, J. W. Andreasen, M. M. Nielsen, M. Giles, M. Heeney, and I. McCulloch, Phys. Rev. B **74**, 115318 (2006).
[9] Y. Kim, S. Cook, S. M. Tuladhar, S. A. Choulis, J. Nelson, J. R. Durrant, D. D. C. Bradley, M. Giles, I. McCulloch, C.-S. Ha, and M. Ree, Nat. Mater. **5**, 197 (2006).
[10] C. Goh, R. J. Kline, M. D. McGehee, E. N. Kadnikova, and J. M. J. Frechet, Appl. Phys. Lett. **86**, 122110 (2005).
[11] H. Sirringhaus, P. J. Brown, R. H. Friend, M. M. Nielsen, K. Bechgaard, B. M. W. Langeveld-Voss, A. J. H. Spiering, R. A. J. Janssen, E. W. Meijer, P. Herwig, and D. M. de Leeuw, Nature (London) **401**, 685 (1999).
[12] S. Hugger, R. Thomann, T. Heinzel, and T. Thurn-Albrecht, Colloid Polym. Sci. **282**, 932 (2004).
[13] H. Yang, T. J. Shin, L. Yang, K. Cho, C. Y. Ryu, and Z. Bao, Adv. Funct. Mater. **15**, 671 (2005).
[14] A. Zen, J. Pflaum, S. Hirschmann, W. Zhuang, F. Jaiser, U. Asawapirom, J. P. Rabe, U. Scherf, and D. Neher, Adv. Funct. Mater. **14**, 757 (2004).
[15] S. Joshi, S. Grigorian, U. Pietsch, P. Pingel, A. Zen, D. Neher, and U. Scherf, Macromolecules **41**, 6800 (2008).
[16] F. C. Spano, J. Chem. Phys. **122**, 234701 (2005).
[17] J. Clark, C. Silva, R. H. Friend, and F. C. Spano, Phys. Rev. Lett. **98**, 206406 (2007).
[18] J. Clark, J.-F. Chang, F. C. Spano, R. H. Friend, and C. Silva, Appl. Phys. Lett. **94**, 163306 (2009).
[19] T. J. Prosa, M. J. Winokur, J. Moulton, P. Smith, and A. J. Heeger, Macromolecules **25**, 4364 (1992).
[20] E. Verploegen, R. Mondal, C. J. Bettinger, S. Sok, M. F. Toney, and Z. Bao, Adv. Funct. Mater. **20**, 3519 (2010).
[21] See Supplemental Material at http://link.aps.org/supplemental/10.1103/PhysRevB.86.205205 for in-depth x-ray diffraction and optical absorption data and analyses.
[22] R. J. Kline, M. D. McGehee, and M. F. Toney, Nat. Mater. **5**, 222 (2006).
[23] S. T. Turner, P. Pingel, R. Steyrleuthner, E. J. W. Crossland, S. Ludwigs, and D. Neher, Adv. Funct. Mater. **21**, 4640 (2011).
[24] J. Gierschner, Y.-S. Huang, B. V. Averbeke, J. Cornil, R. H. Friend, and D. Beljonne, J. Chem. Phys. **130**, 044105 (2009).
[25] J. Rivnay, R. Noriega, R. J. Kline, A. Salleo, and M. F. Toney, Phys. Rev. B **84**, 045203 (2011).
[26] M. Sanyal, B. Schmidt-Hansberg, M. F. G. Klein, C. Munuera, A. Vorobiev, A. Colsmann, P. Scharfer, U. Lemmer, W. Schabel, H. Dosch, and E. Barrena, Macromolecules **44**, 3795 (2011).
[27] D. M. DeLongchamp, B. M. Vogel, Y. Jung, M. C. Gurau, C. A. Richter, O. A. Kirillov, J. Obrzut, D. A. Fischer, S. Sambasivan, L. J. Richter, and E. K. Lin, Chem. Mater. **17**, 5610 (2005).
[28] L. H. Jimison *et al.* (unpublished).
[29] P. K.-H. Ho, L.-L. Chua, M. Dipankar, X. Gao, D. Qi, A. T.-S. Wee, J.-F. Chang, and R. H. Friend, Adv. Mater. **19**, 215 (2007).
[30] T. Kushida, T. Nagase, and H. Naito, Appl. Phys. Lett. **98**, 063304 (2011).
[31] H. Jia, S. Gowrisanker, G. K. Pant, R. M. Wallace, and B. E. Gnade, J. Vac. Sci. Technol. A **24**, 1228 (2006).
[32] R. J. Kline, M. D. McGehee, E. N. Kadnikova, J. Liu, J. M. J. Frechet, and M. F. Toney, Macromolecules **38**, 3312 (2005).
[33] M. Kiguchi, M. Nakayama, K. Fujiwara, K. Ueno, T. Shimada, and K. Saiki, Jpn. J. Appl. Phys. **42**, 1408 (2003).
[34] Z. Q. Li, G. M. Wang, N. Sai, D. Moses, M. C. Martin, M. Di Ventra, A. J. Heeger, and D. N. Basov, Nano Lett. **6**, 224 (2006).
[35] F. Dinelli, M. Murgia, P. Levy, M. Cavallini, F. Biscarini, and D. M. de Leeuw, Phys. Rev. Lett. **92**, 116802 (2004).
[36] O. G. Reid, J. A. N. Malik, G. Latini, S. Dayal, N. Kopidakis, C. Silva, N. Stingelin, and G. Rumbles, J. Polym. Sci. Pol. Phys. **50**, 27 (2012).
[37] M. Brinkmann and P. Rannou, Macromolecules **42**, 1125 (2009).
[38] P. Pingel, A. Zen, R. D. Abellon, F. C. Grozema, L. D. A. Siebbeles, and D. Neher, Adv. Funct. Mater. **20**, 2286 (2010).
[39] B. A. Collins, J. E. Cochran, H. Yan, E. Gann, C. Hub, R. Fink, C. Wang, T. Schuettfort, C. R. McNeill, M. L. Chabinyc, and H. Ade, Nat. Mater. **11**, 536 (2012).